

Implementation of Deep Learning based Automated Diagnosis of Glaucoma Using Digital Retinal Fundus Images

Santhosh S^{1*,2}, D. Veerabhadra Babu³ Dr. Anoop B K⁴

¹Research Scholar, Dept. of CSE, Srinivas University, Mangalore, India. ²Assistant Professor NMAM Institute of Technology, Nitte (Deemed to be University), Udupi, India ³Professor, Dept. of CSE, Srinivas University:: Institute of Engineering & Technology, Mangalore. ⁴Professor, Dept. of AIML, Srinivas Institute of Technology, Mangaluru, India

How to cite this article: Santhosh S, Babu DV, Anoop BK, Implementation of Deep Learning based Automated Diagnosis of Glaucoma Using Digital Retinal Fundus Images, International Journal of Contemporary Medicine, 2023;11(2): 24-30.

Abstract

Glaucoma is a prevalent chronic condition that can cause irreversible vision loss. The number of individuals suffering from permanent vision loss as a result of glaucoma is predicted to rise at an alarming rate in the near future. There is a lot of study being done on computer-aided diagnosis for glaucoma. The optic cup (OC) and optic disc (OD) are typically segmented in retinal fundus images to distinguish between glaucomatous and non-glaucomatous instances. However, the OC boundaries are quite non-distinctive; as a result, accurate OC segmentation is extremely difficult, and OD segmentation performance also needs to be improved. To address this issue, we suggest two networks for accurate glaucoma screening: CNN and RNN-LSTM. We created a CNN-RNN hybrid that extracts not only the spatial information in a fundus image but also the temporal features encoded in fundus sequential images. A CNN and a combined CNN and Long Short-Term Memory RNN were trained using 1810 fundus pictures and 295 fundus videos. In differentiating glaucoma from healthy eyes, the combined CNN/RNN model achieved an average F-measure of 95.2%. In comparison, the fundamental CNN model only achieved an average F-measure of 78.2%. Both proposed networks include a separable convolutional link to improve computational efficiency and lower network costs. The proposed architecture can provide great accuracy even with only a few trainable parameters.

Keywords: Optic cup, optic disc segmentation, Glaucoma screening, Computer-aided diagnosis, convolutional neural networks, Recurrent Neural Network (RNN).

Introduction

This Glaucoma is one of the biggest causes of blindness among eye illnesses, with an estimated 80 million individuals affected by 2020¹. Glaucoma, unlike other eye illnesses such as cataracts and myopia, cannot be reversed. Thus, early screening is critical for early treatment in order to preserve vision and life quality. Many glaucoma patients, however, are unaware of their disease². As illustrated in the bottom row of Fig. 1, glaucoma is often known as the “silent theft of sight.” To screen for glaucoma, three clinical examinations are used: intraocular pressure (IOP) measurement, function-based visual field test,

and optic nerve head (ONH) assessment. IOP is a significant risk factor, but it is not specific enough to be an effective screening tool for the vast majority of glaucoma patients with normal tension. Function-based visual field testing necessitates the use of specialized perimetric equipment that is not typically seen in primary care clinics. Furthermore, early glaucoma frequently lacks visual symptoms. ONH assessment is a simple approach to detect glaucoma early and is now commonly used by skilled glaucoma experts³⁻⁵. Glaucoma optic nerve head damage can be detected utilizing Fundoscopy, visual field assessment, optical coherence tomography, and digital

Corresponding author: Santhosh S, Information Science Department, Faculty of NMAMIT, Nitte (Deemed to be University), Udupi, India.

E-mail: santhosh.s@nitte.edu.in

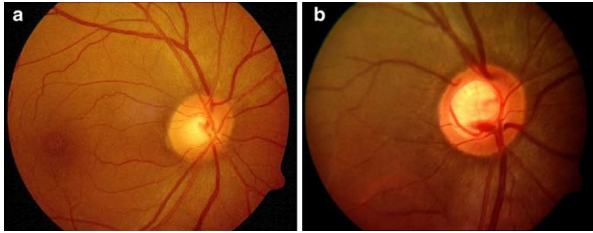


Fig -1: (a) Normal eye fundus image and; (b) glaucomatous.

fundus imaging are examples of clinical tools. Digital fundus images have recently been presented as a viable means of utilizing signal processing and machine learning techniques for the automated assessment of the optic nerve head in a large-scale glaucoma screening scenario due to their non-invasive, cost-effective, and quick nature.

In this study, we describe a three-featured method for computer-based glaucoma detection. The first feature is the cup to disc ratio, which indicates the shift in cup area caused by glaucoma. Glaucoma causes the cup region to expand, causing the optic nerve head to move to the nasal side. This movement in relation to the position of the optic disc center is expressed as a distance. The ratio of this distance to the diameter of the optic disc is the second parameter. The last distinguishing feature is the ratio of total area of blood vessels⁶ in the inferior and superior sides of the optic disc to total area of blood vessels in the nasal and temporal area (ISNT). Deep learning models, particularly convolutional neural networks (CNN), are raising the bar in medical picture processing. These models are being used in a variety of healthcare applications, including dermatologist-level skin cancer categorization⁷ and the detection of pneumonia on chest CT⁹. The main research focus in ophthalmology has been the diagnostic ability of CNNs in the 'big four' eye illnesses (diabetic retinopathy⁸, glaucoma⁹⁻¹¹, using publicly available color fundus photographs and, to a lesser extent, optical coherence tomography (OCT) scans. Deep learning diagnostic models can help overcome the difficulty of glaucoma under

diagnosis while retaining a low false positive rate. Successes in the field of automated glaucoma diagnosis and glaucoma-related metrics from fundus pictures employing CNNs have already been recorded.

Materials and Methods

Fundus photography is the process of obtaining a two-dimensional image of the three-dimensional ocular retinal fundus by projecting reflected light onto an image plane. Table 1 provides an overview of commonly used fundus image datasets used in DL-based diagnosis of the aforementioned retinal disorders. The table displays datasets, the number of fundus images contained inside them, image size, format, and ground truth description. Color-coding is used to show how these datasets can be used for disease diagnosis¹². All datasets are given in one table for ease of comprehension and comparison. The fundus image is a reflection of the internal surface of the eye that is routinely recorded in three colors by image sensors. It contains data about observable biological structures such as the retinal surface, retinal vasculature, the macula, and the optic disc. The blue color's spectral spectrum improves vision of the anterior retinal layers because blood vessels and the posterior retinal pigment layer absorb it. Meanwhile, the green spectrum is reflected by retinal pigmentation¹³, providing more information from beneath the retinal surface and improving retinal layer visualization. The red spectrum contains information concerning choroidal ruptures¹⁴, choroidal nevi, choroidal melanomas, and pigmentary abnormalities, and is only connected to the choroidal layer underlying the pigmented epithelium.

Table 1: Overview of widely used fundus image datasets.

	Glaucoma	Normal
Number of participants	401	387
Male	161	152
Female	250	176
Average age (years, SD)	60	49

Machine Learning Methods

Machine learning refers to techniques that can be implemented in systems designed to solve issues in a variety of sectors. It is divided into two major domains based on the types of target knowledge that must be learnt. Supervised learning occurs when information is explicit or directly human-involved. Otherwise, learning is classified as unsupervised or semi-supervised,¹⁵ depending on how independently the corresponding system judges the target-related pattern without human intervention. Supervised learning methods include k-nearest neighbour (kNN),¹⁶ a support vector machine (SVM), fuzzy techniques, and random forest (RF)¹⁷, whereas unsupervised learning methods include k-means clustering, fuzzy c-means (FCM), the Gaussian mixture model (GMM)¹⁸, and reinforcement learning.

Deep Learning Concepts

Building neural networks for deep learning has recently been considered an efficient way to transform input data to a condensed representation with end-to-end learning among the techniques mentioned above. There are numerous forms for generating neural networks,¹⁹ depending on how the nodes are connected and the fundamental components of the design. A layer is formed by grouping a given number of nodes together, and nodes in the same layer are not normally connected to each other. In terms of neural network building blocks, a fully connected network (FCN) is one in which all nodes²⁰ in one layer are connected to all nodes in the following layer. A convolutional neural network (CNN) is a network that propagates the given information by partially connecting to the nodes of the next layer with regular intervals and the same weights. Finally, if the inference operations are carried out by repeatedly feeding the previous results as inputs, the network is referred to as a recurrent neural network (RNN) and is often built to handle sequential data. The approaches utilized in this work are primarily focused on

deep learning models²¹, as deep learning is a cutting-edge technology that has been shown to outperform traditional machine learning. However, conventional approaches are also covered for certain tasks if their ability to analyze necessary patterns and produce comparable results to deep learning methods

Deep learning is a type of machine learning technique that use deep neural networks to learn various tasks. Convolutional neural networks (CNN) are the most widely used deep learning models for computer vision²² tasks such as medical imaging. Other deep learning methods in development include CNN ensembles, transfer learning, CNN combined with traditional machine learning, fully convolutional neural networks, and auto encoders. In this part, commonly used deep learning architectures²³ and training methods are explored briefly.

Preprocessing

The fundus images used for fine-tuning were automatically cropped around the optic disc using a bounding box 1.5 times the radius of the optic disc. With the exception of the RIMONE database, this was originally cropped around the optic disc. We used the method provided in²⁴ to crop this image. Xu et al. employed a rudimentary CNN to find the most likely pixels in the optic disc region. The candidate pixels are then sorted using a threshold. Cropping images around the optic disc serves a clinical purpose; glaucoma disease primarily affects the optic disc and its environs. Furthermore, Orlando et al.²⁵ demonstrated that cropping images around the optic disc was more efficient than using the entire images when using CNN for glaucoma assessment. Images that were utilized to fine-tune the CNNs.

Training Methods

A neural network is often trained by starting with random weights and tweaking them through stochastic gradient descent and back propagation. The following are some strategies for training a neural network that

have been used in the literature for ophthalmic diagnostics using fundus images. Deep learning techniques typically demand huge datasets for efficient training. The datasets available in ocular diagnosis²⁶ are typically small, which can lead to model overfitting. Transfer learning solves this problem by fitting the weights on a big dataset, frequently from a dissimilar domain. The weights of some or all of the model's layers are then fine-tuned on the target dataset. Ensemble learning entails training several deep learning models independently²⁷ and then polling their results for a given data sample to forecast it. The most prevalent strategy is majority voting, which entails selecting the most frequent result as the final prediction. It is predicated on the premise that the faults of separately trained models are unlikely to coincide.

Architecture

CNNs are composed of two parts: (i) a convolutional layer and a max-pool layer, where the input of each layer is the output of the preceding layer, which serves as a feature extractor, and (ii) a fully connected layer, where the extracted features are categorized. In general, it is a hierarchical feature extractor that maps the intensities of the input images to a feature vector. Because they only have one output neuron for each class, the final layer, the fully connected layer, performs classification followed by logarithmic softmax activation function. All of the parameters have been tweaked to reduce misclassification error over the training set. Figure 2 depicts an overview of our suggested CNN framework. We created a CNN-RNN hybrid that extracts not only the spatial information in a fundus image but also the temporal features encoded in fundus sequential images. A CNN and a combined CNN and Long Short-Term Memory RNN were trained using 1840 fundus pictures and 295 fundus videos²⁸. Bringing together CNN and RNN. To extract spatial and temporal information, we used a mixed CNN and RNN (LSTM) architecture. Figure 2 depicts the broad framework of our method. Each sequential image is transformed

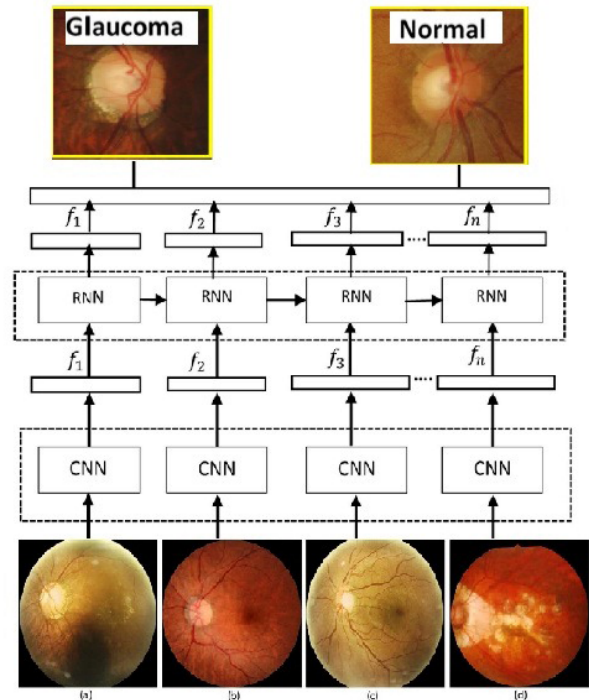


Fig -2: Overall framework of the mixed Convolutional Neural Network-Recurrent Neural Network (CNNRNN).

into another sequential image and fed into the CNN for spatial feature extraction²⁹. The results are then fed into a recurrent sequence learning model (e.g., LSTM) to identify temporal properties in the image sequence. Finally, the combined features are passed on to a fully connected layer, which predicts the classification for the entire input sequence.

Results and Discussion

The photos of the retinal fundus were collected from a publically available source. There are 589 normal photos and 837 glaucoma images in all. All images are captured with a Zeiss FF 450 Fundus camera and converted to jpeg format for further processing. To undertake the systematic evaluation, we resized all of the input fundus images to 64 64 and subjected them to CNN. The entire algorithm is written in MATLAB and ran on a system with an Intel Xeon CPU E3-1225, 3.3 GHz, 16 GB RAM, and a GPU. The first portion of the evaluation uses images of size 64 64 with learning rates of 0.1, 0.01, 0.001, and 0.0 0 01. Following the division of the data set into

training and testing sets, the algorithm is run, and various performance parameters such as accuracy, sensitivity, specificity, and positive predictive value (PPV)³⁰ are computed for evaluation. The best results are obtained with a learning rate of 0.001. We achieved 98.13% accuracy, 98% sensitivity, 98.30% specificity, and 98.79% reliability.

$$\text{Sensitivity} = \text{TP} / (\text{TP} + \text{FN}) \quad (1)$$

$$\text{Specificity} = \text{TN} / (\text{TN} + \text{FP}) \quad (2)$$

$$\text{Accuracy} = (\text{TP} + \text{TN}) / (\text{TP} + \text{FP} + \text{TN} + \text{FN}) \quad (3)$$

CNN architecture for glaucoma CAD using digitized fundus images. Furthermore, our model is robust because it provides consistent performance across all iterations. There are various advantages to employing CNN for automated glaucoma detection. The elimination of traditional steps such as feature extraction, dimensionality reduction, and feature ranking is one of the primary benefits. It automatically extracts features by generating feature maps after each layer and determines the best performing features for itself. This saves a significant amount of time and memory. Another advantage of CNN and RNN-LSTM is that CNN does not require pre-processing steps, which can have an impact on performance. CNN requires a large number of images to work well. It is not possible to generalize the technique using fewer photos. Increasing the number of photos also increases the number of layers, which may increase the algorithm's computing time.

As a result, the model's parameters must be carefully chosen in order to achieve optimal performance in the shortest amount of time. Furthermore, developing the best performing CNN model may take more time. Furthermore, as the number of images increases, it may take longer to converge. To solve this difficulty, we may need to use a graphics processing unit (GPU). Also, in general, CNN is more reliant on training images, and its performance suffers when tested with negative images that do not belong to any of the trained classes. In the future, we plan to enhance this generated CNN model by training modified

images rather than raw images utilising a multi column and multi scale convolutional neural network to detect different phases of glaucoma with a large database. Figure 3 shows an enhanced image using CLAHE in all (RGB) channels. The augmentation is carried out in three picture channels. We can notice the retinal blood vessel in this image because the retinal image background dominates the color and texture information.

For the first time, we show that training a combined CNN and RNN on retinal image sequences can extract both spatial and temporal characteristics, resulting in much enhanced glaucoma identification. More particular, when compared to a base network, the combination CNN and RNN network using LSTM architecture achieved much greater sensitivity and specificity rates.

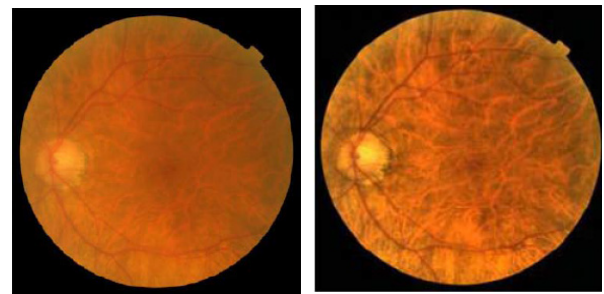


Figure-3: Original and enhanced image using CLAHE.

Table -2: Overview Performance of the various models

Models	Acc	Spec	Sen	F1
CNN	93.21	0.55	0.59	56.4
CNN-RNN	95.11	0.70	0.72	70.3
Proposed Net	95.91	0.79	0.88	83.9



Figure-4: The receiver operating characteristic curves for all the different models.

Conclusions

Deep learning is proposed as a revolutionary strategy for glaucoma diagnosis and prediction in this research. The glaucoma dataset was used to train the deep learning model for glaucoma image analysis. Only about a quarter of the data was used for research purposes. The features were retrieved using DenseNet-201, a pre-trained transfer learning model combined with CNN and RNN-LSTM. A deep convolutional neural network was used to classify the photos in order to diagnose glaucoma. The patient's glaucoma status was determined using these retinal fundus pictures. The optic cup region was extracted from the fundus photographs, and the extracted image data was then compared to the ground truth images in the dataset. In order to organise the data, attributes were extracted from segmented photographs using the DenseNet model. The model was 93.82 percent accurate when used for training and 91.90 percent accurate when tested, according to earlier models. Other models have accuracy differences of 1.36 to 5.26 percentage points. Both the comparison and the training show that this model outperforms earlier models with an Acc of 95.91 when compared to the competition.

ACKNOWLEDGEMENT

I wish to thank my parents for their support and encouragement throughout my study.

CONFLICTS OF INTEREST

The authors declare no conflict of interest.

ETHICS APPROVAL

Not applicable

FUNDING STATEMENT

None.

References

1. Y.-C. Tham, X. Li, T. Y. Wong, H. A. Quigley, T. Aung, and C.-Y. Cheng, "Global prevalence of glaucoma and projections of glaucoma burden through 2040: A systematic review and meta-analysis," *Ophthalmology*, vol. 121, no. 11, pp. 2081-2090, 2014.
2. S. Y. Shen, T. Y. Wong, P. J. Foster, J.-L. Loo, M. Rosman, S.-C. Loon, W. L. Wong, S.-M. Saw, and T. Aung, "The prevalence and types of glaucoma in Malay people: The Singapore Malay Eye Study," *Investigative Ophthalmology and Visual Science*, vol. 49, no. 9, p. 3846, 2008.
3. J. Jonas, W. Budde, and S. Panda-Jonas, "Ophthalmoscopic evaluation of the optic nerve head," *Survey of Ophthalmology*, vol. 43, no. 4, pp. 293-320, 1999.
4. J. E. Morgan, N. J. L. Sheen, R. V. North, Y. Choong, and E. Ansari, "Digital imaging of the optic nerve head: monoscopic and stereoscopic analysis," *British Journal of Ophthalmology*, vol. 89, no. 7, pp. 879-884, 2005.
5. H. Fu, Y. Xu, S. Lin, X. Zhang, D. Wong, J. Liu, and A. Frangi, "Segmentation and Quantification for Angle-Closure Glaucoma Assessment in Anterior Segment OCT," *IEEE Trans. Med. Imag.*, vol. 36, no. 9, pp. 1930-1938, 2017.
6. Fu H, et al. Disc-aware ensemble network for glaucoma screening from fundus image. *IEEE Trans Med Imaging* 2018;37(11):2493-501. <https://doi.org/10.1109/TMI.2018.2837012>. Nov.
7. Parashar D, Agrawal DK. Automated classification of glaucoma stages using flexible analytic wavelet transform from retinal fundus images. *IEEE Sens J* 2020; 20(21):12885-94. <https://doi.org/10.1109/JSEN.2020.3001972>. 1 Nov.1.
8. Civit-Masot J, Domínguez-Morales MJ, Vicente-Díaz S, Civit A. Dual machine learning system to aid glaucoma diagnosis using disc and cup feature extraction. *IEEE Access* 2020;8:127519-29. <https://doi.org/10.1109/ACCESS.2020.3008539>.
9. Roychowdhury S, Koozekanani DD, Kuchinka SN, Parhi KK. Optic disc boundary and vessel origin segmentation of fundus images. *IEEE J Biomed Health Inform* 2016;20(6):1562-74. <https://doi.org/10.1109/JBHI.2015.2473159>. Nov.
10. Guo F, et al. Yanbao: a mobile app using the measurement of clinical parameters for glaucoma screening. *IEEE Access* 2018;6:7741428. <https://doi.org/10.1109/ACCESS.2018.2882946>.
11. Ganesh E, Shanker NR, Priya M. Non-invasive measurement of glaucoma disease at earlier stage through GMR sensor AH biomagnetic signal from eye and RADWT algorithm. *IEEE Sens J* 2019;19(14):540412. <https://doi.org/10.1109/JSEN.2019.2909526>. 15 July15.
12. Juneja M, Thakur S, Wani A, et al. DC-Gnet for detection of glaucoma in retinal fundus imaging. *Mach Vis Appl* 2020;31:34. <https://doi.org/10.1007/s00138-020-01085-2>.
13. de Sousa JA, de Paiva AC, Sousa de Almeida JD, et al. Texture based on geostatistic for glaucoma diagnosis from fundus eye image. *Multimed Tools Appl* 2017;76:19173-90. <https://doi.org/10.1007/s11042-017-4608-y>.
14. Bajwa MN, Malik MI, Siddiqui SA, et al. Two-stage framework for optic disc localization and glaucoma classification in retinal fundus images using deep learning. *BMC Med Inform Decis Mak* 2019;19:136. <https://doi.org/10.1186/s12911-019-0842-8>.

15. Bouacheria M, Cherfa Y, Cherfa A, et al. Automatic glaucoma screening using optic nerve head measurements and random forest classifier on fundus images. *Phys Eng Sci Med* 2020;43:1265–77. <https://doi.org/10.1007/s13246-020-00930-y>.
16. Hirota M, Mizota A, Mimura T, et al. Effect of color information on the diagnostic performance of glaucoma in deep learning using few fundus images. *IntOphthalmol* 2020;40:3013–22. <https://doi.org/10.1007/s10792-020-01485-3>.
17. Vijapur NA, Kunte RSR. Sensitized glaucoma detection using a unique template based correlation filter and undecimated isotropic wavelet transform. *J Med Biol Eng* 2017;37:365–73. <https://doi.org/10.1007/s40846-017-0234-4>.
18. Holden BA, Fricke TR, Wilson DA, et al. Global prevalence of myopia and high myopia and temporal trends from 2000 through 2050. *Ophthalmology*. 2016;123:1036e1042.
19. Weinreb RN, Aung T, Medeiros FA. The pathophysiology and treatment of glaucoma: a review. *JAMA*. 2014;311:1901e1911.
20. Thompson AC, Jammal AA, Medeiros FA. A review of deep learning for screening, diagnosis, and detection of glaucoma progression. *Transl Vis Sci Technol*. 2020;9:42.
21. Tham YC, Li X, Wong TY, et al. Global prevalence of glaucoma and projections of glaucoma burden through 2040: a systematic review and meta-analysis. *Ophthalmology*. 2014;121:2081e2090.
22. Wu JH, Nishida T, Weinreb RN, Lin JW. Performances of machine learning in detecting glaucoma using fundus and retinal optical coherence tomography images: a meta-analysis. *Am J Ophthalmol*. 2022;237:1e12.
23. Christopher M, Belghith A, Bowd C, et al. Performance of deep learning architectures and transfer learning for detecting glaucomatous optic neuropathy in fundus photographs. *Sci Rep*. 2018;8:16685.
24. Liao W, Zou B, Zhao R, Chen Y, He Z, Zhou M. Clinical interpretable deep learning model for glaucoma diagnosis. *IEEE J Biomed Health Inform*. 2020;24:1405e1412.
25. Yu S, Xiao D, Frost S, Kanagasingam Y. Robust optic disc and cup segmentation with deep learning for glaucoma detection. *Comput Med Imaging Graph*. 2019;74:61e71.
26. Wang H, Wang Z, Du M, et al. Score-cam: score-weighted visual explanations for convolutional neural networks. In: *Proceedings of the IEEE/CVF Conference on Computer Vision and Pattern Recognition Workshops*. 2020:24e25.
27. Fu H, Cheng J, Xu Y, Liu J. Glaucoma detection based on deep learning network in fundus image. In: *Deep Learning and Convolutional Neural Networks for Medical Imaging and Clinical Informatics*. Springer; 2019:119e137.
28. Nawaz M, Nazir T, Javed A, et al. An efficient deep learning approach to automatic glaucoma detection using optic disc and optic cup localization. *Sensors*. 2022;22:434.
29. Islam MT, Mashfu ST, Faisal A. Siam, deep learning-based glaucoma detection with cropped optic cup and disc and blood vessel segmentation. *IEEE Access*. 2021;10: 2828e2841.
30. Xu X, Guan Y, Li J, et al. Automatic glaucoma detection based on transfer induced attention network. *Biomed Eng OnLine*. 2021;20:1e19.